Research Article

Journal of Applied Toxicology

Received: 30 August 2013, Revised: 23 September 2013, Accepted: 24 September 2013 Published online in Wiley Online Library

(wileyonlinelibrary.com) DOI 10.1002/jat.2955

Hepatic fibrogenesis and transforming growth factor/Smad signaling activation in rats chronically exposed to low doses of lead

Rossana C. Perez Aguilar†, Stella M. Honoré†, Susana B. Genta and Sara S. Sánchez*

ABSTRACT: Lead is an important heavy metal pollutant in the environment. The nervous system, kidney and liver are the most susceptible organs to lead deposition, showing that this pollutant has no single target system. To examine the cellular and molecular mechanisms involved in their pathobiology of chronic lead at low-dose exposure in the liver, male Wistar rats were exposed to 0.06% lead acetate in drinking water every day for 4 months. At the end of the study, hepatic metal accumulation, morphology and function were examined. Immunochemical staining and Western blot analysis were performed to detect extracellular matrix proteins, α-smooth muscle actin and transforming growth factor (TGF)β1/Smad pathway expression. Results showed increased laminin, collagen IV and fibronectin, located at the perisinusoidal space. Phenotypic transformation of hepatic stellate cells into myofibroblast-like cells was evidenced at the ultrastructural level and a significant expression of α-smooth muscle actin in Disse's space was observed. These findings were associated with a marked increase in TGFβ1/Smad2/3 signaling. Our data suggest that, chronically, exposure to low levels of lead could trigger the onset of a hepatic fibrogenic process through upregulated TGFβ1/Smad signaling. Copyright © 2013 John Wiley & Sons, Ltd.

Keywords: lead; liver; fibrogenesis

Introduction

Lead is a nonessential toxic metal whose widespread use has caused extensive environmental contamination and health problems such as cognitive and behavioral impairment, anemia, gastrointestinal toxicity and chronic renal failure (Ademuyiwa *et al*., 2007; Lanphear *et al*., 2005; Patrick, 2006; Pérez Aguilar *et al*., 2008; Villeda-Hernandez *et al*., 2001). There is growing evidence that levels of lead intake considered innocuous a few years ago could result in subtle noxious effects in both humans and experimental animals (Gilbert and Weiss, 2006; Park *et al*., 2006; Spivey, 2007). Moreover, different studies have confirmed that there does not seem to be a threshold for the toxic effects of lead (Canfield *et al*., 2003; American Academy of Pediatrics, Committee on Environmental Health, 2005; Martin *et al*., 2006).

The liver is one of the major organs involved in the storage, biotransformation and detoxification of toxic substances and is not spared from the noxious of lead (Shaban El-Neweshy and Said El-Sayed, 2011). Several studies have shown that lead affects hepatic enzymes of the drug metabolism, cholesterol and lipid metabolism and oxidative stress, and can cause liver hyperplasia (Ademuyiwa *et al*., 2009; Kojima *et al*., 2004; Massó *et al*., 2007; Pillai and Gupta, 2005). These different effects have been attributed to the toxicokinetics of lead and to the level and duration of metal exposure. However, the mechanism of the effects of this metal on the liver is controversial and not yet clear.

Hepatic fibrosis is a common response to chronic liver injury of variable origin (viral, metabolic or toxic). Regardless of the etiologic factor, liver fibrosis is characterized by increased production of extracellular matrix (ECM) components that form hepatic scars and consists of fibril-forming collagens and matrix glycoconjugates such as laminins, fibronectins and hyaluronic acid (Wynn, 2008).

In normal liver, three cell types are involved in the synthesis and secretion of ECM: hepatocytes, endothelial cells and hepatic stellate cells (HSCs), these nonparenchymal quiescent cells being the primary source of ECM (Clement *et al*., 1986; Friedman, 2000; Gutierrez-Ruiz and Gomez-Quiroz, 2007). Moreover, HSCs store vitamin A and its derivative retinoids and maintain the normal basement membrane-type matrix (Geerts, 2001).

Numerous *in vivo* and *in vitro* studies have shown that when the liver is injured, HSCs undergo a process of activation and differentiate into myofibroblasts (Arnaud *et al*., 2003; Iredale, 2001). Activation of HSCs is characterized by cell enlargement, enhanced proliferation and loss of lipid droplets and retinoids along with increased expression of alpha smooth muscle actin (α-SMA) (Mann and Smart, 2002; Scott and Friedman, 2008). HSCs have been identified as the primary source of excess ECM accumulation in liver fibrosis (Wynn, 2008).

*Correspondence to: Sara S. Sánchez, Dpto. Biología del Desarrollo, INSIBIO (Consejo Nacional de Investigaciones Científicas y Técnicas-Universidad Nacional de Tucumán (CONICET-UNT). Chacabuco 461, T4000ILI San Miguel de Tucumán, Argentina.
E-mail: ssanchez@fbqf.unt.edu.ar

†Both authors contributed equally.

Dpto. Biología del Desarrollo, INSIBIO (Consejo Nacional de Investigaciones Científicas y Técnicas-Universidad Nacional de Tucumán (CONICET-UNT). Chacabuco 461, T4000ILI San Miguel de Tucumán, Argentina

A variety of cytokines is able to modulate the production of matrix proteins. Platelet-derived growth factor is the most potent proliferative cytokine for HSCs, and transforming growth factor-β (TGFβ) is a powerful fibrogenic mediator in a number of diseases (Clouthier *et al*., 1997; Sato *et al*., 2003; Sime *et al*., 1997).

There are three isotypes of TGFβ in mammals, TGFβ1, -2 and −3, all exhibiting a similar biological activity (Gorelik and Flavell, 2002). Although a variety of cell types produce and respond to TGFβs (Letterio and Roberts, 1998; Wells, 2000), tissue fibrosis is primarily attributed to the TGFβ1 isoform (De Bleser *et al*., 1997; Massagué, 2000).

TGFβ1 initiates its cellular effects by binding to high-affinity cell transmembrane receptors, including type I and type II TGFβ receptors (TGFRI and TGFRII). The TGFRI complex triggers signaling intermediates known as Smad proteins. Smad is the condensation of the names of the signaling molecules identified downstream of TGFβ superfamily ligand in *Drosophila* (Mad) and *Caenorhabditis elegans* (Sma) (Roberts *et al*., 2003). As the important members of the TGFβ/Smad signaling pathway, activated Smad2 and Smad3 proteins transduce signals directly from the cell membrane to the nucleus and mediate intracellular TGFβ1 signal transduction, regulating cell proliferation, transformation, apoptosis, synthesis and secretion of ECM (Breitkopf *et al*., 2006; Honoré *et al*., 2012; Kamato *et al*., 2013).

In this paper, we investigated the mechanisms of long-term low-level lead doses in promoting hepatic fibrogenesis. We analyzed the cells, the ECM components and TGFβ1/Smad signaling as one of the mechanisms involved in the onset of a fibrogenic process in a lead-exposed liver.

Materials and Methods

Experimental animals

Male Wistar rats weighing ~ 200–220 g were obtained from the animal facility of the INSIBIO (Instituto Superior de Investigaciones Biológicas, San Miguel de Tucumán, Argentina). The animals had not been subjected to previous experimental procedures. All animals were housed at constant temperature (22 °C) under a 12: 12 h light–dark cycle, with free access to a standard laboratory chow. The following experiments were conducted in agreement with the Guide for the Care and Use of Laboratory Animals (Institute of Laboratory Animal Resources, Commission on Life Sciences, National Research Council, National Academy Press, Washington, DC), and the local Institutional Animal Care Committee.

An *in vivo* animal model of chronic lead toxicity was applied. Animals were randomly divided into an experimental and a control group of 10 animals each. Animals in the experimental group were given 0.06% lead acetate in their drinking water for 4 months. After preliminary assays with different doses of lead acetate (0.01%, 0.06% and 0.1%), 0.06% was chosen on the basis that it caused blood lead levels to reach values within biological tolerance values (BAT). BAT was defined as the maximum permissible quantity of a chemical substance or its metabolites or the maximum permissible deviation from the norm of biological parameters induced by lead in exposed humans. (Drexler *et al*., 2008; Pérez Aguilar *et al*., 2008). The controls received ordinary tap water throughout the experimental period.

At the end of the experimental period, the animals were weighed and killed under anesthesia (i.p. ketamine–xylazine 50: 5 mg kg^{-1} body weight). Livers were removed, weighed and observed macroscopically and then analyzed microscopically.

Blood samples

Blood was collected by cardiac puncture in heparinized tubes for lead analysis. Lead was determined in the whole blood using an Atomic Absorption Spectrometer (Perkin-Elmer AAnalyst 600, Perkin Elmer Co, California, USA) with a graphite furnace. Blood for hematological studies was collected into tubes containing ethylenediaminetetraacetic acid anticoagulant. The blood hemoglobin level (g dl^{-1}) was measured by optical density at 540 nm using Drabkin's (cyanmethemoglobin) reagent. Other red blood cell indices were measured according to standard procedures using a Cell-Dyn 3700 (Abbott Diagnostics, Santa Clara, CA, USA) hematology analyser. Blood for clinical chemistry studies was collected into tubes without anticoagulant, allowed to clot and centrifuged to obtain serum. To assess the degree of liver damage the plasma enzymatic activity of alanine aminotransferase (ALT), aspartate aminotransferase (AST) and gamma glutamyl transferase (γGT) and plasma protein were measured using an Alcyon Analyser ISE (Abbott) and Axsym™ System (Abbott).

Urine samples

One day before being killed, the rats were individually placed in metabolic cages during the day and 24 h urine samples were collected. These samples were allowed to stand at 4 °C in the dark until analysis. δ-aminolevulinic acid dehydratase (δ-ALAD) activity was assayed according to the method of Tomokuni and Ogata (1972). 2-Methyl-3-carbethoxy-4-(3-propionic acid) pyrrole, produced by the condensation of δ-ALA acid with ethyl acetoacetate, was determined using a modified Ehrlich's reagent at 555 nm.

Histological studies

Samples of fresh liver tissue were rinsed with ice-cold phosphate-buffered saline (PBS, pH 7.4), immersed in Bouin's fixative overnight at 4 °C and then embedded in paraplast. Thick sections (4 μm) were cut from the blocks and stained with hematoxylin–eosin and Mallory's triple stain methods to evaluate histopathological changes in the livers. Liver changes were determined in cross-sections by analysis of adjacent microscope fields throughout the length of the tissue pieces. This represented at least 40 nonadjacent microscope fields (approximately 8.5 mm) in each tissue The study was performed in a blinded manner in nonadjacent stained sections obtained at 50 μm intervals using an Olympus BX80 fluorescence microscope.

Transmission electron microscopy

For electron microscope examination, thin sections of livers were fixed for 4 h at 4 °C in 4% glutaraldehyde and 0.1% sodium phosphate (pH 7.4). Afterwards, specimens were washed twice in phosphate buffer and post-fixed in 1% osmium tetroxide in the same buffer at 4 °C overnight. Samples were dehydrated in an ethanol series and embedded in Spurr resin. Ultrathin sections were carried out with a Potter Blum MT1 ultramicrotome (MT1, Sorval Porter Blum, USA). Slices were stained with lead citrate and uranyl acetate and examined with a Zeiss EM 109 electron microscope (Zeiss, Oberkochen, Germany).

Journal of Applied Toxicology

Sodium dodecyl sulfate–polyacrylamide gel electrophoresis and Western immunoblotting procedure

As previously described (Sánchez *et al*., 2001), for the sodium dodecyl sulfate–polyacrylamide gel electrophoresis (SDS-PAGE) and immunoblotting procedure livers were homogenized at 4 °C in extraction buffer (50 mmol l^{-1} Tris–HCl, pH 7.4, 0.1 mol l^{-1} NaCl and 1% Nonidet P-40) containing the following protease inhibitors: 2 mmol l^{-1} phenylmethylsulfonyl fluoride (Sigma-Aldrich Chemical Co., St. Louis, MO, USA), 0.5 μg ml^{-1} leupeptin (Sigma-Aldrich), 5 μg ml^{-1} pepstatin (Sigma-Aldrich) and 5 μg ml^{-1} aprotinin (Sigma-Aldrich). Then, the extracts were centrifuged at 10 000 *g* for 15 min. Lipids were extracted from the supernatant as described by Heifetz and Snyder (1981) by adjusting the sample to 10: 10: 3 (v/v/v) chloroform–methanol–water. Precipitated proteins were solubilized in sample buffer for SDS–PAGE. Protein concentration of each sample was determined by Lowry's procedure (Lowry *et al*., 1951). Samples were boiled in 2% SDS, 2% 2-mercaptoethanol, 20 mmol l^{-1} Tris–HCl, pH 7, for 3 min.

Denaturing PAGE was carried out following Laemmli's procedure (1970). Equal quantities of SDS-denatured proteins (20 μg $lane^{-1}$) were electrophoresed in 5 and 7.5 % polyacrylamide gels. The molecular weights of the denatured samples were estimated from a calibration curve obtained with the standard proteins in a prestained SDS–PAGE standard solution (Sigma-Aldrich). The gels were stained with Coomassie Blue R-250. After SDS–PAGE, the immunoblotting analyses were performed according to the method of Towbin (1979). Electrophoresed proteins were transferred from the gel to a nitrocellulose membrane rinsed with distilled water and blocked with 3% bovine serum albumin in phosphate buffer saline (BSA–PBS) for 1 h at room temperature. Dilutions of polyclonal antibody to human plasma fibronectin or of polyclonal antibody to laminin-1 or of monoclonal anticollagen type IV clone COL-94 were added and incubated overnight al 4 °C (specific antibodies and dilutions used are listed in Table 1). Then the membranes were rinsed three times with PBS for 10 min with gentle shaking. The antigen–antibody reaction was detected using biotin-conjugated secondary antibodies and ExtrAvidin Peroxidase conjugates (Sigma-Aldrich); each of them was diluted and the membranes were incubated for 2 h at room temperature. After each incubation, the membranes were rinsed three times with PBS for 10 min each time. Peroxidase activity was detected by incubating blots with 3,3′-diaminobenzidine–H_2O_2 (Sigma-Aldrich). The relative intensities to protein bands were measured and normalized to the intensity of γ-tubulin using the Image J 1.44 software (NIH Image).

Indirect immunohistochemical staining

Immunoperoxidase labeling

Paraffin-embedded sections (5 μm) were dried overnight at 37 °C and then deparaffinized and rehydrated. The sections were incubated with 0.3% H_2O_2 in methanol for 30 min to inactivate endogenous peroxidase and treated with 0.1% Trypsin (Merck KgaA, Darmstadt, Germany) for 10 min at room temperature to unmask antigenic sites. Nonspecific staining was blocked by 3% BSA supplemented with 10% (w/v) normal goat serum for 1 h, and then incubated with primary antibodies at 4 °C overnight (see Table 1).

After rinsing with PBS, the sections were treated with biotinylated secondary antibodies for 2 h at room temperature and with ExtrAvidin-Peroxidase conjugate for 2 h at room temperature. Peroxidase activity was detected by incubation with 3,3′-diaminobenzidine–H_2O_2 in the same conditions for 10 min. The reaction was stopped by rinsing with distilled water and slices were mounted in DePex (Hopkins and Williams Ltd., Chadwell Health, UK).

Control procedure for immunostaining, consisted of the omission of the primary antibody or in the substitution of the primary antibody by the corresponding nonimmune sera or normal mouse IgG, were invariably negative (data not shown). Experiments were performed at least three times with similar results and representative images are shown.

Immunofluorescent labeling

After three washes in PBS the liver sections were incubated with 3% BSA supplemented with 10% (w/v) normal goat serum for 1

Table 1. Antibodies

Primary antibody	Host	Dilutiona	Catalogue	Source
α-SMA	Mouse	1:50	A2547	Sigma
Collagen IV	Mouse	1:50	C1926	Sigma
Laminin-1	Rabbit	1:100	L9393	Sigma
Fibronectin	Rabbit	1:100	F3648	Sigma
TGFβ1	Rabbit	1:50	sc-146	Santa Cruz Biotech
TGFβRI	Rabbit	1:50	sc-398	Santa Cruz Biotech
TGFβRII	Rabbit	1:50	sc-400	Santa Cruz Biotech
p-Smad2/3	Goat	1:100	sc-11769	Santa Cruz Biotech
γ-Tubulin	Rabbit	1:100	T3320	Sigma
Secondary antibody				
Biotinylated antigoat IgG	Rabbit	1:750	B7014	Sigma
Biotinylated antimouse IgG	Goat	1:750	B2010	Sigma
Biotinylated antirabbit IgG	Mouse	1:250	B3275	Sigma
Alexa Fluor 488 anti-mouse IgG	Rabbit	1:1500	A11001	Invitrogen
Alexa Fluor 594 anti-rabbit IgG	Goat	1:1500	A21207	Invitrogen
ExtrAvidin®- peroxidase		1:3000	E2886	Sigma

[a]Dilution used in immunohistochemical and immunofluorescence studies.

h at room temperature; slides were then incubated overnight at 4 °C with the primary antibodies. The antibodies used in this study showed highly restricted binding specificities (see Table 1). The specimens were mounted with Glycerol Gelatin (Sigma-Aldrich) and observed with an Olympus BX80 fluorescence microscope.

Double immunostaining

For double-labeled sections, primary antibodies were mixed and incubated as a cocktail. After three washes in PBS, incubation with the secondary Alexa Fluor 488 and Alexa Fluor 594 antibodies (Invitrogen™ Life Technologies, California, USA) was performed (1 h, at room temperature) (see Table 1). The sections were then washed five times in PBS and mounted in aqueous mounting medium with antifading agents (Biomeda, Foster, CA, USA). All secondary antibodies were confirmed to be species-specific for their individual primary antibody. Control sections, which included omission of the primary antibody or the substitution of the primary antibody by the corresponding non-immune sera or normal mouse IgG, were invariably negative. Double-immunolabeled sections were examined by laser scanning confocal microscopy with an Olympus FV300 instrument equipped with multi-line Argon laser (457 nm, 488 nm, 515 nm), argon laser (488 nm), HeNe-Green laser (543 nm) and HeNe-Red laser (633 nm) fitted with the appropriate filter blocks. Linear modulation of brightness and contrast was achieved on the obtained images using Adobe PhotoShop 7.0.

Statistical analysis

Data are presented as means ± SEM. Significant differences between groups were tested by analysis of variance (ANOVA) and Student's *t* test and a $P < 0.05$ was considered statistically significant.

Results

General condition

Animals that received 0.06% lead acetate in drinking water for 4 months presented higher blood lead concentration levels than those of controls (35.90 ± 1.18 vs. 2.12 ± 0.71 μg dl^{-1}, $P < 0.05$).

Continuous lead exposure for 4 months did not cause mortality in rats. Indeed, during the experimental period, the animals appeared normal in their cage. Individual observation outside the cage showed good general condition in lead-exposed animals, without adverse symptoms related to an abnormal autonomic central activity and behavior.

At the end of the experimental period, the body weight of lead-exposed rats was significantly different with respect to that of the control rats ($P < 0.05$) (Table 2). However, no significant change in the liver/body weight ratio was observed in lead-treated rats compared with the controls (Table 2). Macroscopic liver examination revealed no alterations attributable to lead exposition. In the present study, lead administration caused no effect on daily standard rodent diet consumption compared with the control group (18.2 ± 0.3 vs. 18.7 ± 0.2 g).

Biochemical parameters

No significant changes in hematological parameters were noticed at the end of the experimental period in lead-exposed rats compared with control rats (Table 3). However, lead-exposed animals presented a significant increase in urinary δ-ALA acid compared with controls (1.55 ± 0.82 vs. 0.48 ± 0.04 mg g^{-1}, $P < 0.05$).

Table 2. Clinical parameters

Parameter	Control	Lead-treated
Body weight (g)	408.0 ± 15.2	323.0 ± 10.9*
Liver weight (g)	16.2 ± 1.98	13.5 ± 3.21
Liver weight/body weight (%)	3.5 ± 0.6	4.0 ± 0.8

The data are expressed as means ± SEM, $n = 10$ animals.
* Significant differences in lead-treated group compared to the control were $P < 0.05$.

Histological and ultrastructural analysis

In control livers, hematoxylin–eosin staining revealed a normal lobular architecture with a central vein and hepatocytes radially arranged in cords (Fig. 1A). In contrast, lead-exposed livers had irregularly distributed hepatocytes without characteristic cord disposition (Fig. 1B, arrows). However, the morphology of the parenchymal cells did not exhibit changes substantially different from those of the control animals and nuclei were preserved in size and shape. The most important morphological changes were observed at the level of the perisinusoidal spaces, which appeared dilated and showed the presence of fibroblast-like cells, characterized by their typical elongated nuclei. We did not observe any mononuclear or polymorphonuclear cells infiltrating the perisinusoidal spaces (Fig. 1B). The perisinusoidal spaces filled with extracellular proteins were easily identified by the increased intensity of aniline-blue in triple Mallory stain (Fig. 1D,F, arrows).

The ultrastructural analysis by transmission electron microscopy revealed that control hepatocytes presented round clear nuclei (Fig. 2A). The cytoplasms were characterized by an elevated number of large mitochondria surrounded by abundant rough endoplasmic reticulum in close contact with them. Transverse sections of the smooth endoplasmic reticulum associated with glycogen granules and characteristic lysosomes were observed (Fig. 2B). HSCs appeared in contact with hepatocytes. They showed a characteristic nonproliferative phenotype, with tight nuclear chromatin peripherally disposed, and contained several fat droplets that occupied the larger part of the cytoplasm (data not shown).

Sections of lead-exposed livers showed hepatocytes with central nuclei and the characteristic nucleoli (Fig. 2C). However, heterochromatin was more condensed than that in control animals and the presence of granular inclusion bodies inside the nuclei was also observed (Fig. 2E, arrowhead). Abundant electron-dense and dilated mitochondria were observed at the cytoplasm with the presence of vacuolar inclusions with electron-dense contents that probably correspond to lead deposits in the hepatic tissue (Fig. 2F) and cytoplasm fibrillar inclusions (Fig. 2D). Lead-exposed livers showed cells with ultrastructural characteristics of activated HSCs. These cells exhibited a significant loss of fat droplets. They appeared elongated, with irregular cytoplasmic processes of dendritic configuration such as myofibroblasts. The presence of a large amount of extracellular materials such as collagen was observed near the myofibroblastic cells at the perisinusoidal spaces (data not shown).

Journal of Applied Toxicology

Table 3. Hematological and biochemical parameters

Parameters	Control	Lead-treated
Red blood cells (10^{12} l^{-1})	8.25 ± 0.86	8.35 ± 0.44
Hemoglobin (g dl^{-1})	14.90 ± 0.77	15.00 ± 0.63
Hematocrit (%)	75.50 ± 5.77	76.30 ± 2.87
Mean corpuscular volume [MCV] (fL)	91.70 ± 3.18	91.50 ± 2.08
Mean corpuscular hemoglobin [MCH] (pg)	18.10 ± 1.32	18.00 ± 0.18
Mean corpuscular hemoglobin concentration [MCHC] (%)	19.70 ± 0.79	19.70 ± 0.35
Leukocytes (10^{9} l^{-1})	4.84 ± 1.09	4.70 ± 1.10
Platelets (10^{9} l^{-1})	130.00 ± 17.90	149.00 ± 32.00
ALT (UI ml^{-1})	61.9 ± 8.2	77.0 ± 22.8
AST (UI ml^{-1})	145 ± 40.3	149 ± 94.2
γGT (UI ml^{-1})	5.6 ± 2.9	7.3 ± 3.9
Total proteins (mg dl^{-1})	6.98 ± 1.01	6.69 ± 1.10
Creatinine (mg dl^{-1})	0.69 ± 0.15	0.70 ± 0.06
Urea (mg dl^{-1})	46.8 ± 10.3	47.0 ± 13.8

The data are expressed as means ± SEM, $n = 10$ animals. Significant differences in lead-treated group compared to the control were $P > 0.05$.

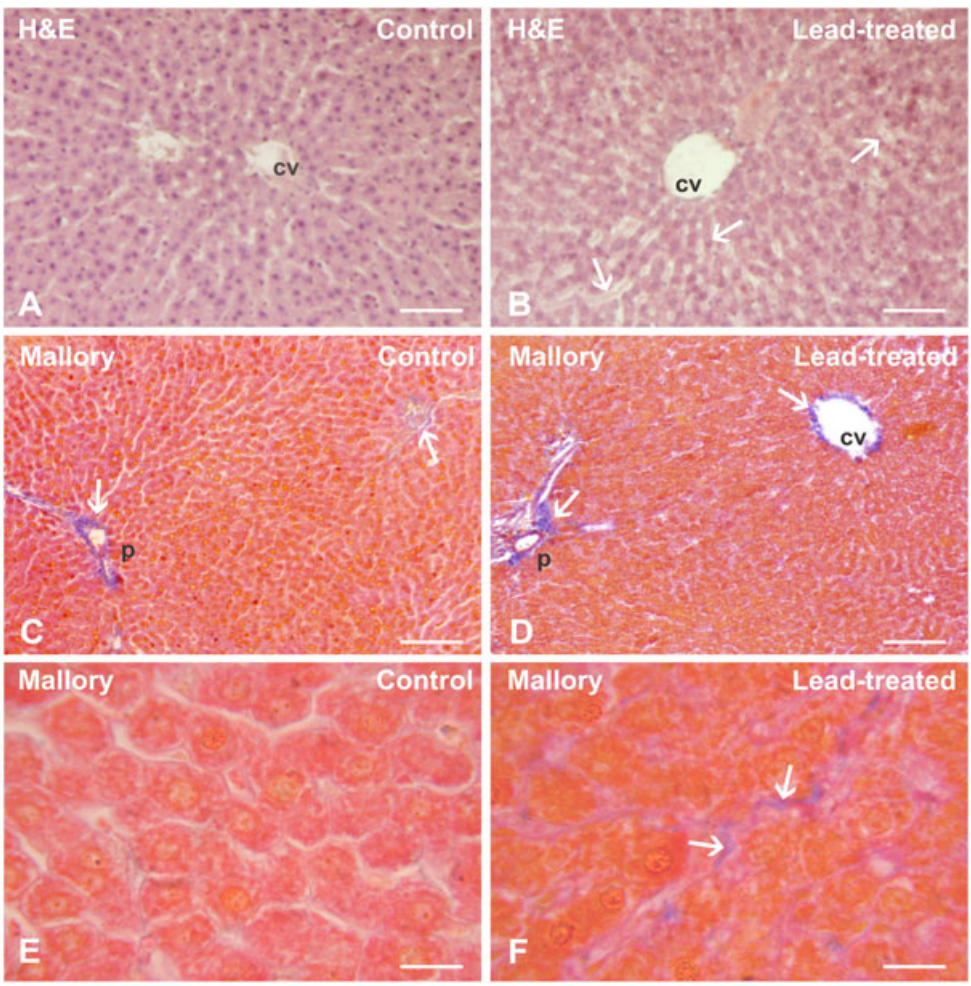

Figure 1. H&E and Mallory's triple staining of liver sections. H&E stained sections (A,B). (A) Normal histoarchitecture and cordonal parenchymal organization arranged radially from the central vein can be observed. (B) Lead-exposed liver shows an irregular arrangement of the hepatic cords with dilated perisinusoidal space (arrows). Mallory's triple staining (C–F). (C) Control liver showing tenuous blue staining in perisinusoidal spaces. (D) Intense blue staining in portal area and central vein of exposed livers (arrows). (E) A weak blue mark is observed delineating hepatocyte cords. (F) Lead-treated liver showing instense blue staining in perisinusoidal spaces (arrows). Bar: (A,B) 50 μm; (C–F) 25 μm. Photographs are representative of all sections studied. cv, central vein; H&E, hematoxylin–eosin; ps, perisinusoidal space.

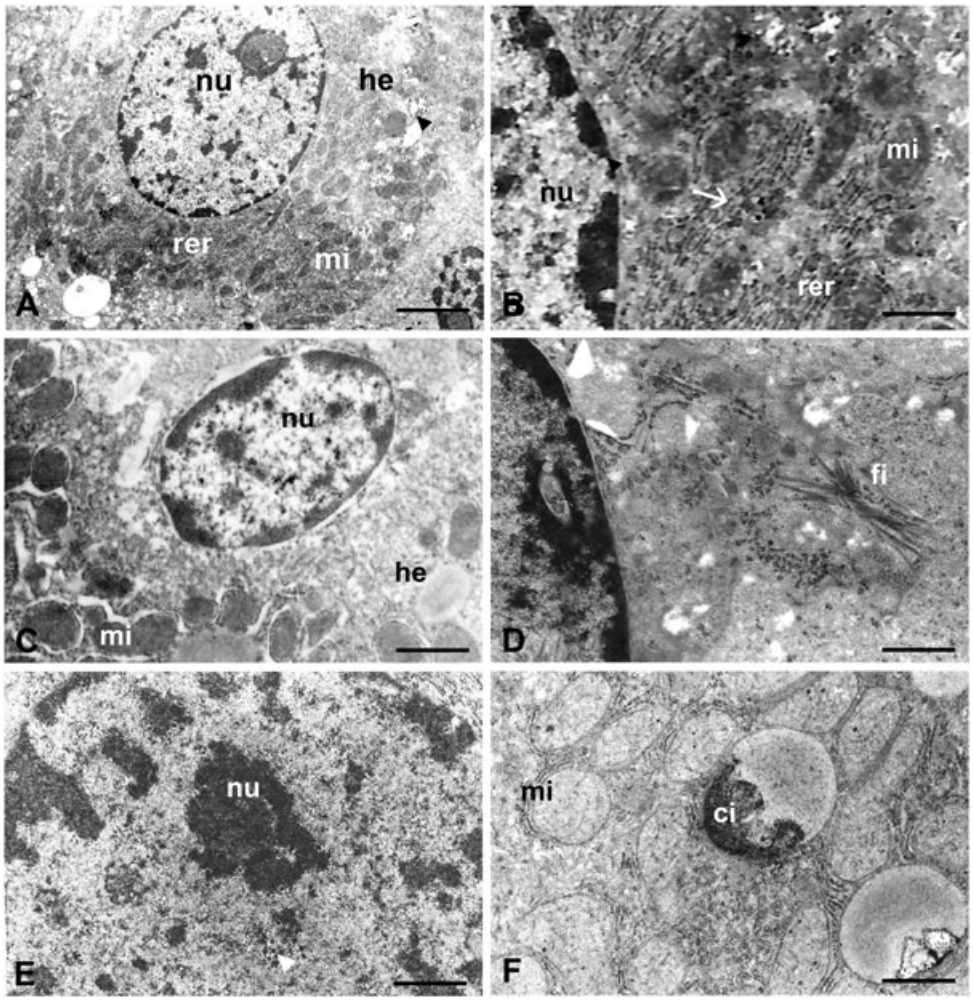

Figure 2. Electron micrograph of control livers and livers exposed to lead acetate. (A) In control livers note hepatocytes with euchromatic nucleus, numerous mitochondria, abundant rough endoplasmic reticulum and glycogen granules (arrowhead). (B) Magnification micrograph showing cytoplasm with rough endoplasmic reticulum, mitochondria, lysosomes and glycogen (arrow). (C) Hepatocyte of exposed liver showing central nucleus with heterochromatin adjacent to the nuclear envelope and larger and more electrondense mitochondria. (D) Magnification micrographs show cytoplasmic fibrillar inclusions. (E) Lead-exposed hepatocyte; note the presence in the nucleus of punctuate inclusions (arrowhead). (F) In exposed liver section cytoplasmic vacuolar inclusions with electron-dense content were evident. Bar: (A,C) 3 μm; (B,D,E,F) 0.9 μm. ci, cytoplasmic vacuolar inclusions with electron-dense content; fi, fibrillar inclusions; he, hepatocyte; lis, lysosomes; nu, nucleus; mi, mitochondria; rer, rough endoplasmic reticulum.

Extracellular matrix deposition in the liver tissue

To determine the expression of collagen IV, laminin-1 and fibronectin in control and lead-exposed livers, tissue extracts were subjected to immunostaining and Western immunoblotting analysis (Fig. 3).

Extracellular protein immunostaining was, in general, stronger in the exposed livers. Laminin-1 was sparsely distributed on the liver parenchyma of control livers and was mainly expressed in the perisinusoidal space (Fig. 3A). However, in lead-exposed livers, laminin-1 was markedly deposited in these areas (Fig. 3B). In control rats, fibronectin was limited to a dashed line outlining the central vein and the hepatocyte cord (Fig. 3C), whereas large amounts of fibronectin were present at the perisinusoidal space in exposed livers (Fig. 3D). Collagen IV immunostaining revealed a weak or absent staining on the liver parenchyma of control livers (Fig. 3E) but strong staining was observed at the perisinusoidal space of exposed livers (Fig. 3F).

Corresponding to these results, blot densitometric analyses revealed an increase in laminin-1 (3.7-fold), fibronectin (4-fold) and collagen IV (2.8-fold) of exposed livers compared with the controls ($P < 0.05$) (Fig. 3I).

Activation of local fibroblasts in liver

Activated HSCs, recognized by their α-SMA immunoreactivity, play a pivotal role in the pathogenesis of fibrocontractive changes in the liver. In the control group, scarce or no α-SMA-positive staining was found along the sinusoids. It mostly appeared in the peripheral zones of the hepatic lobule close to the portal spaces and around the central veins (Fig. 3G). In the lead-exposed group, α-SMA expression was greatly elevated and mainly detected along the sinusoids at the perisinusoidal space, where the myofibroblastic cells were located (Fig. 3H).

As shown in Fig. 4(A–C), both α-SMA and fibronectin were colocalized in the perisinusoidal area and around the central vein (yellow stain) of exposed livers. These findings suggest that activated HSCs could be the cellular source of increased fibronectin in the perisinusoidal space.

Journal of Applied Toxicology

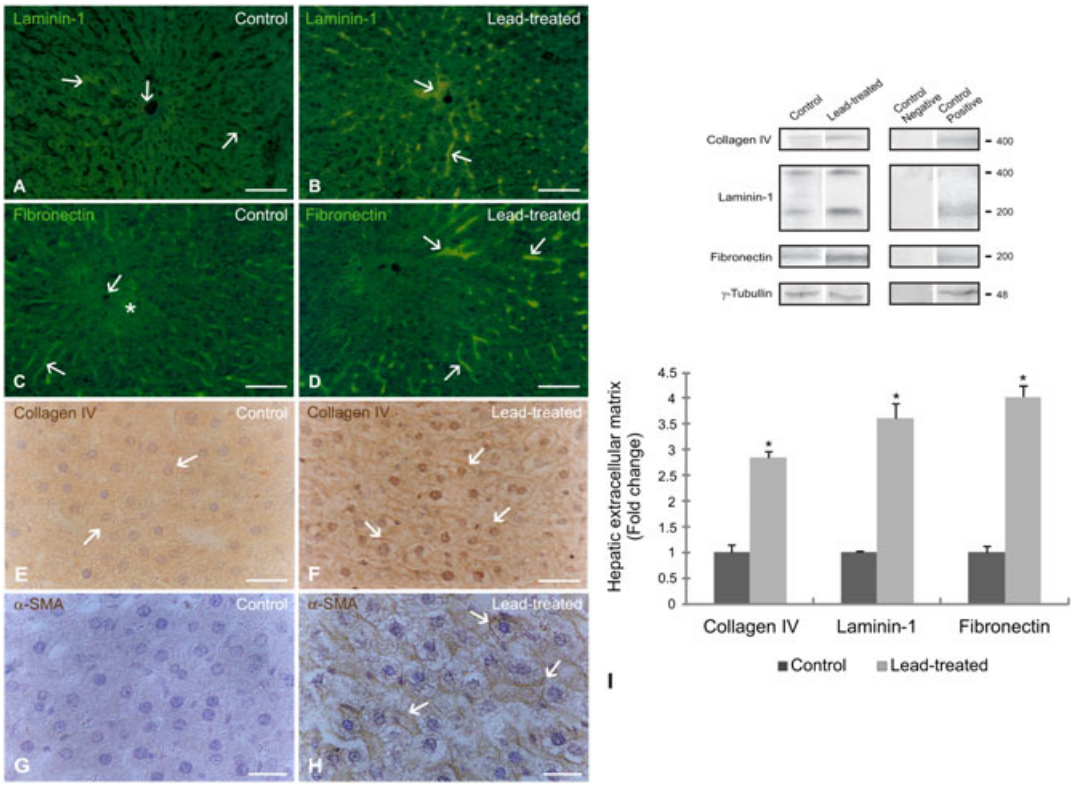

Figure 3. Collagen IV, laminin-1, fibronectin and α-SMA expression in control and lead-exposed livers. (A) Immunolocalization of laminin-1 in control sections. A weak staining is observed in the perisinusoidal matrix (arrow). (B) In lead-exposed liver strong immunoreactivity (arrow) can be observed at the perisinusoidal space. (C) Control sections showing a weak staining around the central vein (arrow) and in some hepatocytes (asterisk). (D) Lead-exposed liver showing intense immunoreactivity to fibronectin at perisinusoidal spaces. Photographs are representative of all sections studied. (E) A weak staining for collagen IV can be observed in control liver parenchyma. (F) Note strong staining for collagen IV at the perisinusoidal space of exposed livers (arrows). (G) Control liver shows no anti-α-SMA reactivity in perisinusoidal spaces. (H) In liver sections of exposed rats, note the intense anti-α-SMA immunoreactivity along the perisinusoidal spaces (arrow) and cells α-SMA + (arrowhead). Photographs are representative of all sections studied. Bar: (A–D) 50 μm; (E–H) 25 μm. (I) Western blotting of collagen IV, laminin and fibronectin from control and lead liver extracts. Relative mean protein levels of collagen IV, laminin and fibronectin from control and lead liver extracts are shown in representative Western blot bands. Molecular weights (kDa) are indicated to the right. Negative technical controls: omission of primary antibody. Positive technical controls: intestinal homogenates. A total of three independent experiments were performed. Data are normalized to control results for each experiment and represented as means ± SEM; $*P < 0.05$; $n = 3$ in each group. SMA, alpha smooth muscle actin.

Transforming growth factor pathway

We next determined whether morphological changes seen in the lead-exposed livers were associated with altered TGFβ1/Smad signaling. As shown in Fig. 5 ligand TGFβ1, receptors TGFβ RI and TGFβ RII, and downstream signaling protein phosphorylated-Smad2/3 (p-Smad2/3) were weakly expressed in control livers. However, lead-exposed livers showed strong TGFβ1 and p-Smad2/3 expression.

Figure 5A revealed a weak or absent immunostaining of TGFβ1 on the control liver parenchyma. In contrast, exposed livers showed a strong expression of the ligand on hepatocyte surfaces adjacent to the perisinusoidal space. TGFβ1 immunoreactivity was also detected in the hepatocyte cytoplasms, possibly due to the presence of its precursor protein (pro-TGFβ1), which is also recognized by the antibody (Fig. 5B).

Control sections showed a weak immunoreactivity for TGFRI and TGFRII at the hepatocytes cell membrane (Fig. 5C,E). Unlike the control livers, both receptors evidenced increased staining in the exposed livers. TGFRI and TGFRII were located mainly on the surface of hepatocytes and perisinusoidal liver cells (Fig. 5D,F).

Control liver tissue was practically devoid of p-Smad2/3 immunostaining. Lead-exposed livers presented p-Smad2/3 staining mainly in the nucleus of hepatocytes and in the perinuclear area (asterisk). Besides, in some hepatocytes stippled marks in the cytoplasms (arrow) were observed (Fig. 5G). Interestingly, in contrast to control livers, the perisinusoidal space of lead-exposed sections presented positive immunoreactivity to p-Smad2/3 in close contact with the parenchymal cells (arrowhead) (Fig. 5H).

Western blot analyses revealed a single band of 12 kDa corresponding to TGFβ1 in both animal groups (Fig. 5I). A fourfold increase in TGBβ1 expression in exposed livers compared with controls ($P < 0.05$) was observed. As shown in Fig. 5I, the expression of TGFRI and TGFRII receptors was higher than that in unexposed control animals (1.5- and 1.3-fold increase respectively; $P < 0.05$). Analysis of phosphorylated Smads (p-Smad2/3) showed an immunoreactive band of 55 kDa in both groups. Interestingly, the results revealed a significant increase (2.20-fold) in the homogenates of exposed livers compared to the controls ($P < 0.05$) (Fig. 5I).

Discussion

Environmental and occupational heavy metal pollution are frequent problems in both developing and industrialized countries. Lead intoxication is one of the most common forms of metal

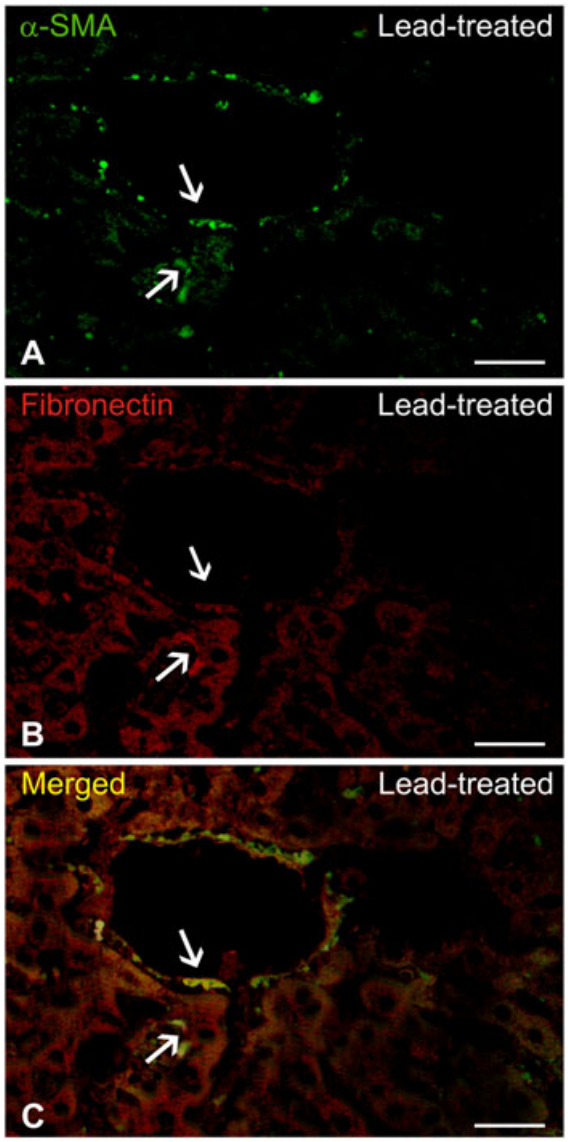

Figure 4. Double-labeling immunohistochemistry for α-SMA and fibronectin in lead-exposed liver sections. (A) Liver sections immunolabeled with anti α-SMA (green). (B) In the same sections, immunodetection of fibronectin (red). (C) Colocalization of both markers. Note overlapped immunolabeling (yellow) in muscle cells present in the central vein and other cells in close contact with the hepatocytes surfaces (arrow). Bar: 25 μm. SMA, alpha smooth muscle actin.

intoxication. Numerous studies in humans and animals indicate that high levels of lead exposure can promote renal, nervous, hepatic, hematological and reproductive disorders (Ashry *et al.*, 2010; El-Sayed and El-Neweshy, 2010; Flora *et al.*, 2008). However, the effects of chronic low-level lead exposure have not been well-studied.

In the present work, we evaluated the biological effects of 0.06% lead acetate on the liver. Traditionally, lead poisoning was considered when classical symptoms were present with high blood lead levels. However, it is recognized that blood lead levels are poor indicators of body lead burden and only reflect recent exposure (Loghman-Adham, 1997). Our findings demonstrate that lead hepatotoxicity even occurs in the absence of symptoms or with minimal biochemical changes at the cellular and molecular levels.

Several enzymatic processes responsible for heme synthesis can be used as biomarkers for the toxic effects of lead, primarily δ-ALAD, which catalyzes the condensation of two molecules of 5-aminolevulinic acid to form the heme precursor, porphobilinogen. As the activity of δ-ALAD is inhibited by lead binding, this enzyme is accepted as the most sensitive measurable biological index of lead toxicity (Barbosa *et al.*, 2005; Tomokuni *et al.*, 1993). In our experimental model, low lead level exposure produced an increase in urinary δ-ALA, even though blood biological tolerance values were present in the animals (Drexler *et al.*, 2008).

Liver damage caused by lead exposure used to be considered a rare event; however, in recent years, hepatotoxicity studies increased and new evidence of lead pathophysiology was presented (Mudipalli, 2007). Nevertheless, results in human or animal models are controversial (Herman *et al.*, 2009; Pande *et al.*, 2001; Singh *et al.*, 1994; Teijón *et al.*, 2006). The current study revealed that low-level lead acetate exposure in drinking water for 4 months did not result in important functional changes in the liver.

Liver enzymes γGT, ALT and AST are used as biomarkers to test liver function and hepatic integrity (Rahmioglu *et al.*, 2009). Damage to the hepatocyte membrane will cause the release of many of these enzymes into the circulating blood. In our experimental model, no significant changes were found in the serum levels of γGT, ALT or AST. These results were further supported by our histopathological study, where no severe hepatocyte damage or necrosis were observed after lead ingestion. In agreement with our findings, Teijón *et al.* (2006) and Herman *et al.* (2009) showed that rats exposed to low lead concentrations did not present significant alterations in hepatic enzyme activities. For these authors, the normality of these parameters was probably due to a process of metabolic adaptation to the exposure conditions.

Histological evaluation showed only a moderate disruption of normal hepatic architecture induced by lead acetate. Nevertheless, the most significant changes were evidenced at the perisinusoidal space with increased deposition of ECM and the emergence of α-SMA positive fibroblast-like cells. Moreover, the ultrastructural study revealed morphological changes in HSCs with loss of cytoplasmic lipid droplets and change of quiescent phenotype to a myofibroblastic-like appearance in chronic low lead-exposed rats. This phenotypic change is known as HSC activation (Friedman, 2004; Wells, 2006).

Several etiologic agents are able to induce HSC activation. Among them, we can mention hepatitis C virus, excessive consumption of alcoholic beverages, nonalcoholic steatohepatitis, cytokines and reactive oxygen species, carbon tetrachloride and iron (Bataller and Brenner, 2005; Clément *et al.*, 2010; Nagano *et al.*, 2007; Neubauer *et al.*, 1999; Pinzani *et al.*, 2005; Zhang *et al.*, 2006). The present study, for the first time, provides evidence that low levels of lead exposure induce HSC activation.

Activation of HSCs is the central event in the early stages of hepatic fibrosis (Hinz *et al.*, 2007; Reeves and Friedman, 2002). These perisinusoidal cells orchestrate an array of changes, including degradation and deposition of the normal ECM. HCS cells transformed into myofibroblast-like cells acquire contractile capacity, migrate to injury sites and secrete large amounts of ECM components as well as a wide range of proinflammatory cytokines and fibrogenic mediators (Amuddu *et al.*, 2007; Gressner and Weiskirchen, 2006; Wells, 2006).

In our experimental model, lead produced changes in the expression of ECM components in the liver of exposed animals, showing a significant increase in laminin, collagen type IV and

Journal of Applied Toxicology

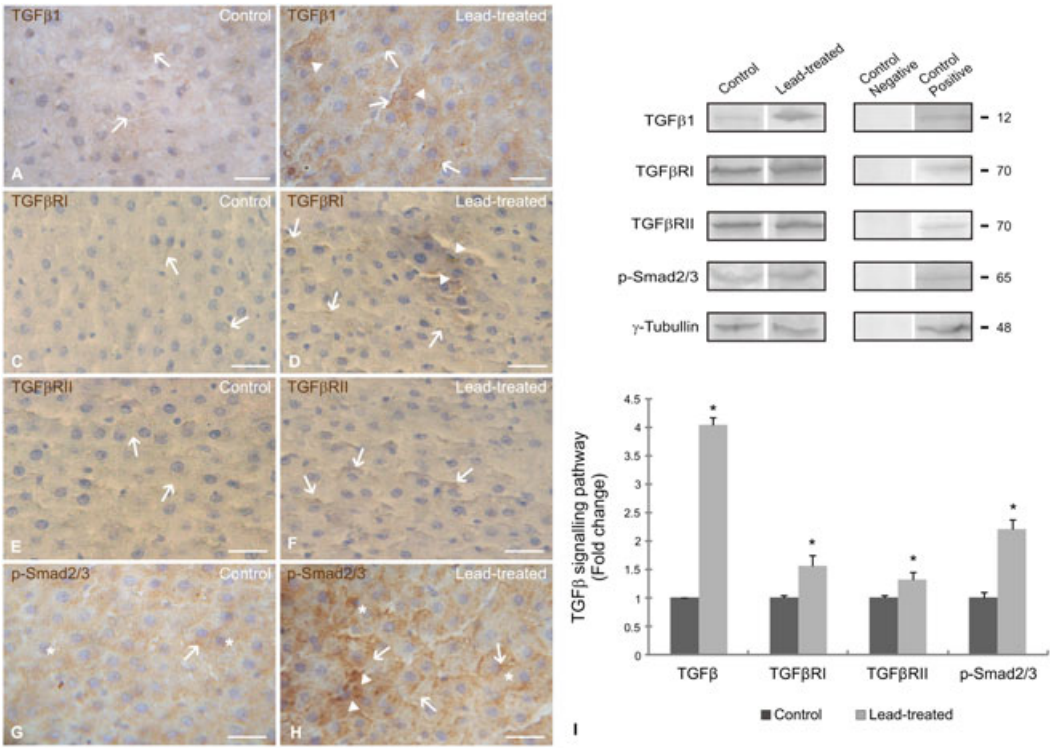

Figure 5. TGFβ, TGFβRI, TGFβRII and p-Smad2/3 expression in control and lead-exposed livers. (A) Weak positive immunostaining for TGFβ1 in liver sections of control animals. (B) Intense immunoreactivity to TGFβ1 (arrows) at the cytoplasm and perisinusoidal space (arrowhead) sections of lead-exposed livers. (C) Weak immunoreactivity to TGFβRI receptor (arrow) in control livers. (D) Positive immunostaining to TGFβRI present in the area facing the perisinusoidal space (arrow) of lead-exposed liver sections. Note the myofibroblast-like cells located in the perisinusoidal space with positive marks for TGFβRI (arrowhead). (E) Weak positive immunoreactivity to TGFβRII receptor is observed in control sections (arrow). (F) Intense reactivity to TGFβRII (arrow) in the area facing the perisinusoidal space in lead-exposed livers. (G) Weak immunoreactivity to p-Smad 2/3 in the cytoplasm (arrow) and nucleus (asterisk) of control hepatocytes. (H) Strong immunoreactivity to cytoplasm (arrow) and nucleus (asterisk) is observed in lead-exposed livers. Note at perisinusoidal space the positive marks to p-Smad 2/3 (arrowhead). Bar: 25 μm. Photographs are representative of all sections studied. (I) Western blotting of TGFβ, TGFβRI, TGFβRII and p-Smad2/3 from control and lead 0.06% liver extracts. Representative blots of TGFβ, TGFβRI, TGFβRII and p-Smad2/3 and γ-tubulin. The molecular weights (kDa) of detected protein bands are indicated to the right. Negative controls: omission of primary antibody. Positive controls: intestinal homogenates. Histograms present in arbitrary units the densitometric analysis of the bands with respect to γ-tubulin. Values are means ± SEM, $n = 3$ animals. *Significantly different from control group $P < 0.05$. TGF, transforming growth factor.

fibronectin. The secretion of these molecules resulted in an increase in ECM deposition. It has been shown that, in normal liver, the ECM occupies a very limited compartment (less than 3% of the total tissue) and is restricted to the portal area, central vein and sinusoidal walls (Bedossa and Paradis, 2003). However, in certain pathological conditions such as chronic viral hepatitis and nonalcoholic steatosis, accumulation of ECM proteins modifies Disse's space and leads to disorders in hepatic architecture and fibrotic scar formation (Guo and Friedman, 2007). In our model, the increased expression of extracellular molecules at the perisinusoidal spaces could be considered as a cause of dilated Disse's space.

Coincident fibronectin and α-SMA expression at the perisinusoidal space allow us to suggest that HSCs could be the main source of this major component of hepatic ECM. Nonparenchymal liver cells are now generally considered the primary source of ECM in normal and fibrotic liver, although hepatocytes have also been suggested to contribute to ECM production (Wells, 2008). However, in other hepatotoxicity models such as in CCl4-induced liver fibrosis and in experimental biliary fibrosis, increasing amounts of extracellular proteins transcripts were demonstrated in HSCs but not in hepatocytes, confirming that HCSs produce matrix components (Ramadori and Saile, 2004).

Although increased collagen accumulation is the hallmark of fibrosis, it has been recognized that fibronectin occurs early, preceding the deposition of collagen and persisting with high levels in advanced fibrosis (George *et al*., 2000; Odenthal *et al*., 1992; Wallace *et al*., 2008). Thus, fibronectin plays an important structural role, as it would allow the polymerization of fibrillar collagen and the formation of fibrous networks (Sottile and Hocking, 2002; Velling *et al*., 2002). Different variants of cellular fibronectin are expressed during an inflammatory response or tissue injury (Saito *et al*., 1999). *In vitro* studies suggest that the concerted action of fibronectin and TGFβ, a potent fibrogenic mediator, are required for the phenotypic transformation of HSCs (Serini *et al*., 1998; Hinz *et al*., 2007). Our results demonstrated that lead exposure produced an increased expression of TGFβ1 and its receptors TGFRI and TGFRII in the liver parenchyma. Gressner and Weiskirchen (2006) established that hepatic TGFβ1 produced by hepatocytes, platelets, Kupffer cells or sinusoidal endothelial cells is involved in HSC activation, α-SMA expression and ECM deposition (Pohlers *et al*., 2009). Experimental evidence showed that TGFβ1 could be produced by active myofibroblasts (Clouthier *et al*., 1997). Gressner (1995) established that activated HSCs generate TGFβ1 as an autocrine form; thus, this molecule regulates its own synthesis and the expression of its cellular receptors.

As mentioned above, experimental evidence exists, showing that Smad3 is the predominant mediator of fibrogenic TGFβ downstream signaling (Breitkopf *et al*., 2006; Roberts *et al*., 2003). In our experimental conditions, we also observed an increase in phosphorylated Smad2/3 proteins, allowing us to suggest that the TGFβ1/Smad2/3 route is upregulated in the liver of lead-exposed animals. Similar results were observed in different experimental models of hepatic fibrosis (Neumann *et al*., 2008; Parkes and Templeton, 2003; Spee *et al*., 2006; Xu *et al*., 2010). Moreover, it has been described that TGFβ1 pathway inhibition leads to a reversal in a fibrotic process previously triggered by overactivation of this pathway (Chen and Lau, 2009; Jiang *et al*., 2004; Kisseleva and Brenner, 2007; Otogawa *et al*., 2008).

In our experimental conditions, increased TGFβ1/Smad2/3 signaling could be related to a pro-oxidative environment promoted by lead (Jurczuk *et al*., 2007; Sivaprasad *et al*., 2004). In this regard, accumulating evidence has shown that lead causes oxidative stress by inducing the generation of reactive oxygen species, including hydroperoxides, singlet oxygen, hydrogen peroxide and superoxide (Jurczuk *et al*., 2007; Sivaprasad *et al*., 2004; Zhang *et al*., 2004). Moreover, by altering or participating in diverse signaling pathways such as TGFβ1 signaling, reactive oxygen species may have significant pathological consequences (Poli, 2000; Forman *et al*., 2003). However, this point requires further studies.

In conclusion, the present work describes the role of lead in promoting liver fibrogenesis and suggests mechanisms in the underlying process. Our results report for the first time, that chronic exposure to low doses of lead could trigger the phenotypic transformation of HSCs, secretion of the ECM and upregulated expression of TGFβ1/Smad signaling. Taken together, these results suggest a role of lead in promoting a fibrogenic state with altered hepatic structure.

Acknowledgements

This research was supported by Consejo Nacional de Investigaciones Científicas y Técnicas (CONICET) and Consejo de Investigaciones de la Universidad Nacional de Tucumán (CIUNT), Argentina, grants to S.S.S. S.S.S. and S.M.H. are Career Investigators of CONICET (Argentina).

Conflict of Interest

The authors did not report any conflict of interest.

References

Ademuyiwa O, Ugbaja RN, Rotimi SO, Abam E, Okediran BS, Dosumu OA, Onunkwor B. 2007. Erythrocyte acetylcholinesterase activity as a surrogate indicator of lead-induced neurotoxicity in occupational lead exposure in Abeokuta, Nigeria. *Environ. Toxicol. Pharmacol.* **24**:183–188.

Ademuyiwa O, Agarwal R, Chandra R, Behari JR. 2009. Lead-induced phospholipidosis and cholesterogenesis in rat tissues. *Chem. Biol. Interact.* **179**:314–320.

American Academy of Pediatrics, Committee on Environmental Health. 2005. Lead exposure in children: Prevention, detection, and management. *Pediatrics* **116**:1036–1046.

Amuddu AK, Guha IN, Elsharkawy AM, Mann DA. 2007. Resolving fibrosis in the diseased liver: translating the scientific promise to the clinic. *Int. J. Biochem. Cell Biol.* **39**:695–714.

Arnaud A, Fontana L, Angulo AJ, Gil A, López Pedrosa JM. 2003. Proliferation, functionality and extracellular matrix production of hepatocytes and a liver stellate cell line. *Dig. Dis. Sci.* **48**:1406–1413.

Ashry KM, El-Sayed YS, Khamiss RM, El-Ashmawy IM. 2010. Oxidative stress and immunotoxic effects of lead and their amelioration with myrrh (Commiphora molmol) emulsion. *Food Chem. Toxicol.* **48**:236–241.

Barbosa F Jr, Tanus-Santos JE, Gerlach RF, Parsons PJ. 2005. A critical review of biomarkers used for monitoring human exposure to lead: advantages, limitations, and future needs. *Environ. Health Perspect.* **113**(12):1669–1674.

Bataller R, Brenner DA. 2005. Liver fibrosis. *J. Clin. Invest.* **115**:209–218.

Bedossa P, Paradis V. 2003. Liver extracellular matrix in health and disease. *J. Pathol.* **200**:504–515.

Breitkopf K, Godoy P, Ciuclan L, Singer MV, Dooley S. 2006. TGF-beta/Smad signaling in the injured liver. *Z. Gastroenterol.* **44**:57–66.

Canfield RL, Henderson CR Jr, Cory-Slechta DA, Cox C, Juskota TA, Lamphear BP. 2003. Intellectual impairment in children with blood lead concentrations below 10 microg per deciliter. *N. Engl. J. Med.* **348**:1517–1526.

Chen CC, Lau LF. 2009. Functions and mechanisms of action of CCN matrix cellular proteins. *Int. J. Biochem. Cell Biol.* **41**:771–783.

Clement B, Grimaud JA, Campion JP, Deugnier Y, Guillouzo A. 1986. Cell types involved in collagen and fibronectin production in normal and fibrotic human liver. *Hepatology* **6**:225–234.

Clément S, Pascarella S, Conzelmann S, Gonelle-Gispert C, Guilloux K, Negro F. 2010. The hepatitis C virus core protein indirectly induces alpha-smooth muscle actin expression in hepatic stellate cells via interleukin-8. *J. Hepatol.* **52**:635–643

Clouthier DE, Comerford SA, Hammer RE. 1997. Hepatic fibrosis, glomerulosclerosis, and a lipodystrophy-like syndrome in PEPCK-TGFβ1 transgenic mice. *J. Clin. Invest.* **100**:2697–2713.

De Bleser PJ, Niki T, Rogiers V, Geerts A. 1997. Transforming growth factor-beta gene expression in normal and fibrotic rat liver. *J. Hepatol.* **26**:886–893.

Drexler H, Göen T, Schaller KH. 2008. Biological tolerance values: change in a paradigm concept from assessment of a single value to use of an average. *Int. Arch. Occup. Environ. Health* **82**:139–142.

El-Sayed YS, El-Neweshy MS. 2010. Impact of lead toxicity on male rat reproduction at "hormonal and histopathological levels". *Toxicol. Environ. Chem.* **92**(4):765–774.

Flora SJS, Mittal M, Mehta A. 2008. Heavy metal induced oxidative stress & its possible reversal by chelation therapy. *Indian J. Med. Res.* **128**:501–523.

Forman HJ, Torres M, Fukuto J. 2003. *Signal Transduction by Reactive Oxygen and Nitrogen Species: Pathways and Chemical Principles*. Kluwer Academic: Boston, MA.

Friedman SL. 2000. Molecular regulation of hepatic fibrosis, an integrated cellular response to tissue injury. *J. Biol. Chem.* **275**:2247–2250.

Friedman SL. 2004. Mechanism of disease: mechanisms of hepatic fibrosis and therapeutic implications. *Nat. Clin. Pract. Gastroenterol. Hepatol.* **1**:98–105.

Geerts A. 2001. History heterogeneity developmental biology and functions of quiescent hepatic stellate cells. *Semin. Liver Dis.* **21**:311–335.

George J, Wang SS, Sevcsik AM, Sanicola M, Cate RL, Koteliansky VE, Bissell DM. 2000. Transforming growth factor-beta initiates wound repair in rat liver through induction of the EIIIA-fibronectin splice isoform. *Am. J. Pathol.* **156**:115–124.

Gilbert SG, Weiss B. 2006. A rationale for lowering the blood lead action level from 10 to 2 mg/dl. *Neurotoxicology* **27**:693–701.

Gorelik L, Flavell RA. 2002. Transforming growth factor-β in T-cell biology. *Nat. Rev. Immunol.* **2**:46–53.

Gressner AM. 1995. Cytokines and cellular crosstalk involved in the activation of fat-storing cells. *J. Hepatol.* **22**(Suppl):28–36.

Gressner AM, Weiskirchen R. 2006. Modern pathogenetic concepts of liver fibrosis suggest stellate cells and TGF-beta as major players and therapeutic targets. *J. Cell. Mol. Med.* **10**:76–99.

Guo J, Friedman SL. 2007. Hepatic fibrogenesis. *Semin. Liver Dis.* **27**:413–426.

Gutierrez-Ruiz MC, Gomez-Quiroz LE. 2007. Liver fibrosis: searching for cell model answers. *Liver Int.* **27**:434–439.

Heifetz A, Snyder JM. 1981. The effects of hydrocortisone on the biosynthesis of sulfated glycoconjugates by human fetal lung. *J. Biol. Chem.* **256**:4957–4967.

Herman DS, Geraldine M, Venkatesh T. 2009. Influence of minerals on lead-induced alterations in liver function in rats exposed to long-term lead exposure. *J. Hazard. Mater.* **166**:1410–1414.

Hinz B, Phan SH, Thannickal VJ, Galli A, Bochaton-Piallat ML, Gabbiani G. 2007. Biological perspectives: The myofibroblast one function, multiple origins. *Am. J. Pathol.* **170**:1807–1816.

Journal of Applied Toxicology

Honoré SM, Cabrera WM, Genta SB, Sánchez SS. 2012. Protective effect of yacon leaves decoction against early nephropathy in experimental diabetic rats. *Food Chem. Toxicol.* **50**(5):1704–1715.

Iredale JP. 2001. Hepatic stellate cell behavior during resolution of liver injury. *Semin. Liver Dis.* **21**: 427–436.

Jiang W, Yang CQ, Liu WB, Wang YQ, He BM, Wang JY. 2004. Blockage of transforming growth factor beta receptors prevents progression of pig serum-induced rat liver fibrosis. *World J. Gastroenterol.* **10**:1634–1638.

Jurczuk M, Moniuszko-Jakoniuk J, Brzóska MM. 2007. Hepatic and renal concentrations of vitamins E and C in lead- and ethanol-exposed rats. An assessment of their involvement in the mechanisms of peroxidative damage. *Food Chem. Toxicol.* **45**:1478–1486.

Kamato D, Burch ML, Piva TJ, Rezaei HB, Rostam MA, Xu S, Zheng W, Little PJ, Osman N. 2013. Transforming growth factor-β signalling: Role and consequences of Smad linker region phosphorylation. *Cell. Signal.* **25**(10):2017–2024.

Kisseleva T, Brenner DA. 2007. Role of hepatic stellate cells in fibrogenesis and the reversal of fibrosis. *J. Gastroenterol. Hepatol.* **22**(Suppl):S73–S78.

Kojima M, Masui T, Nemoto K, Degawa M. 2004. Lead nitrate-induced development of hypercholesterolemia in rats: sterol-independent gene regulation of hepatic enzymes responsible for cholesterol homeostasis. *Toxicol. Lett.* **154**:35–44.

Laemmli UK. 1970. Cleavage of structural proteins during the assembly of the head of bacteriophage T4. *Nature* **227**:680–685.

Lanphear BP, Hornung R, Khoury J, Yoltoon K, Baghurst P, Bellinger DC, Canfield R, Dietrich KN, Bornschein R, Greene T, Rothernber J, Needleman HL, Schnass L, Wasserman G, Graziano J, Roberts R. 2005. Low level environmental lead exposure and children's intellectual function: an international pooled analysis. *Environ. Health Perspect.* **113**:894–899.

Letterio JJ, Roberts AB. 1998. Regulation of immune responses by TGFβ. *Annu. Rev. Immunol.* **16**:137–161.

Loghman-Adham M. 1997. Renal effects of environmental and occupational lead exposure. *Environ. Health Perspect.* **105**:928–939.

Lowry OH, Rosebrough NJ, Farral AL, Randall RJ. 1951. Protein measurement with the Folin phenol reagent. *J. Biol. Chem.* **193**:265–275.

Mann DA, Smart DE. 2002. Transcriptional regulation of hepatic stellate cell activation. *Gut* **50**:891–896.

Martin D, Glass TA, Bandeen-Roche K, Todd AC, Shi W, Schwartz BS. 2006. Association of blood lead and tibia lead with blood pressure and hypertension in a community sample of older adults. *Am. J. Epidemiol.* **163**:467–478.

Massagué J. 2000. How cells read TGF-beta signals. *Nat. Rev. Mol. Cell Biol.* **1**:169–178.

Massó EL, Corredor L, Antonio MT. 2007. Oxidative damage in liver after perinatal intoxication with lead and/or cadmium. *J. Trace Elem. Med. Biol.* **21**:210–212.

Mudipalli A. 2007. Lead hepatotoxicity & potential health effects. *Indian J. Med. Res.* **126**:518–527.

Nagano K, Umeda Y, Saito M, Nishizawa T, Ikawa N, Arito H, Yamamoto S, Fukushima S. 2007. Thirteen-week inhalation toxicity of carbon tetrachloride in rats and mice. *J. Occup. Health* **49**:249–259.

Neubauer K, Krüger M, Quondamatteo F, Knittel T, Saile B, Ramadori G. 1999. Transforming growth factor-beta1 stimulates the synthesis of basement membrane proteins laminin, collagen type IV and entactin in rat liver sinusoidal endothelial cells. *J. Hepatol.* **31**:692–702.

Neumann S, Kaup FJ, Beardi B. 2008. Plasma concentration of transforming growth factor-beta1 and hepatic fibrosis in dogs. *Can. J. Vet. Res.* **72**:428–431.

Odenthal M, Neubauer K, Baralle FE, Peters H, Meyer zum Buschenfelde KH, Ramadori G. 1992. Rat hepatocytes in primary culture synthesize and secrete cellular fibronectin. *Exp. Cell Res.* **203**: 289–296.

Otogawa K, Ogawa T, Shiga R, Nakatani K, Ikeda K, Nakajima Y, Kawada N. 2008. Attenuation of acute and chronic liver injury in rats by iron-deficient diet. *Am. J. Physiol. Regul. Integr. Comp. Physiol.* **294**:R311–R320.

Pande M, Mehta A, Pant B, Flora SJ. 2001. Combined administration of a chelating agent and an antioxidant in the prevention and treatment of acute lead intoxication in rats. *Environ. Toxicol. Pharmacol.* **9**:173–184.

Park SK, Schwartz J, Weisskopf M, Sparrow D, Vokonas PS, Wright RO, Coull B, Nie H, Hu H. 2006. Low-level lead exposure, metabolic syndrome, and heart rate variability: the VA normative aging study. *Environ. Health Perspect.* **114**:1718–1724.

Parkes JG, Templeton DM. 2003. Modulation of stellate cell proliferation and gene expression by rat hepatocytes: effect of toxic iron overload. *Toxicol. Lett.* **144**:225–233.

Patrick L. 2006. Lead toxicity, a review of the literature. Part I: Exposure, evaluation and treatment. *Altern. Med. Rev.* **11**:2–22.

Pérez Aguilar R, Genta S, Sánchez S. 2008. Renal gangliosides are involved in lead intoxication. *J. Appl. Toxicol.* **28**:122–131.

Pillai A, Gupta S. 2005. Antioxidant enzyme activity and lipid peroxidation in liver of female rats co-exposed to lead and cadmium: effects of vitamin E and Mn2+. *Free Radic. Res.* **39**:707–712.

Pinzani M, Rombouts KS. Colagrande S. 2005. Fibrosis in chronic liver diseases: diagnosis and management. *J. Hepatol.* **42** (Suppl. 1): S22–S36.

Pohlers D, Brenmoehl J, Löffler I, Müller CK, Leipner C, Schultze-Mosgau S, Stallmach A, Kinne RW, Wolf G. 2009. TGF-beta and fibrosis in different organs -molecular pathway imprints. *Biochim. Biophys. Acta* **1792**:746–756.

Poli G. 2000. Pathogenesis of liver fibrosis: role of oxidative stress. *Mol. Aspects Med.* **21**:49–98.

Rahmioglu N, Andrew T, Cherkas L, Surdulescu G, Swaminathan R, Spector T, Ahmadi KR. 2009. Epidemiology and genetic epidemiology of the liver function test proteins. *PLoS ONE* **4**(2):e4435.

Ramadori G, Saile B. 2004. Portal tract fibrogenesis in the liver. *Lab. Invest.* **84**:153–159.

Reeves HL, Friedman SL. 2002. Activation of hepatic stellate cells – a key issue in liver fibrosis. *Ront. Biosci.* **7**:d808–d826.

Roberts AB, Russo A, Felici A, Flanders KC. 2003. Smad3: a key player in pathogenetic mechanisms dependent on TGFβ. *Ann. NY Acad. Sci.* **995**:1–10.

Saito S, Yamaji N, Yasunaga K, Saito T, Matsumoto S, Katoh M, Kobayashi S, Masuho Y. 1999. The fibronectin extra domain A activates matrix metalloproteinase gene expression by an interleukin-1-dependent mechanism. *J. Biol. Chem.* **274**:30756–30763.

Sánchez S, Pérez Aguilar R, Genta S, Aybar M, Villecco E, Sánchez Riera A. 2001. Renal extracellular matrix alterations in lead-treated rats. *J. Appl. Toxicol.* **21**:417–423.

Sato M, Muragaki Y, Saika S, Roberts AB, Ooshima A. 2003. Targeted disruption of TGFβ1/Smad3 signalling protects against renal tubulointerstitial fibrosis induced by unilateral ureteral obstruction. *J. Clin. Invest.* **112**:1486–1494.

Scott L, Friedman SL. 2008. Hepatic stellate cells: protean, multifunctional, and enigmatic cells of the liver. *Physiol. Rev.* **88**:125–172.

Serini G, Bochaton-Piallat ML, Ropraz P, Geinoz A, Borsi L, Zardi Gabbiani G. 1998. The fibronectin domain ED-A is crucial for myofibroblastic phenotype induction by transforming growth factor-beta1. *J. Cell Biol.* **142**:873–881.

Shaban El-Neweshy M, Said El-Sayed Y. 2011. Influence of vitamin supplementation on lead-induced histopathological alterations in male rats. *Exp. Toxicol. Pathol.* **63**:221–227.

Sime PJ, Xing Z, Graham FL, Csaky KG, Gauldie J. 1997. Adeno-vector-mediated gene transfer of active transforming growth factor-β1 induces prolonged severe fibrosis in rat lung. *J. Clin. Invest.* **100**:768–776.

Singh B, Dhawan D, Nehru B, Garg ML, Mangal PC, Chand B, Trehan PN. 1994. Impact of lead pollution on the status of other trace metals in blood and alterations in hepatic functions. *Biol. Trace Elem. Res.* **40**:21–29.

Sivaprasad R, Nagaraj M, Varalakshmi P. 2004. Combined efficacies of lipoic acid and 2,3-dimercaptosuccinic acid against lead-induced lipid peroxidation in rat liver. *J. Nutr. Biochem.* **15**:18–23.

Sottile J, Hocking DC. 2002. Fibronectin polymerization regulates the composition and stability of extracellular matrix fibrils and cell-matrix adhesions. *Mol. Biol. Cell* **13**(10):3546–3559.

Spee B, Arends B, van den Ingh TS, Brinkhof B, Nederbragt H, Ijzer J, Roskams T, Penning LC, Rothuizen J. 2006. Transforming growth factor beta-1 signalling in canine hepatic diseases: new models for human fibrotic liver pathologies. *Liver Int.* **26**:716–725.

Spivey A. 2007. The weight of lead. Effects add up in adults. *Environ. Health Perspect.* **115**:A31–A36.

Teijón C, Olmo R, Blanco D, Romero A, Teijón JM. 2006. Low doses of lead: effects on reproduction and development in rats. *Biol. Trace Elem. Res.* **111**:151–165.

Tomokuni K, Ogata M. 1972. Simple method for determination of urinary delta-aminolevulinic acid as an index of lead exposure. *Clin. Chem.* **18**(12):1534–1536.

Tomokuni K, Ichiba M, Fujishiro K. 1993. Interrelation between urinary delta-aminolevulinic acid (ALA), serum ALA, and blood lead in workers exposed to lead. *Ind. Health* **31**:51–57.

Towbin H, Staehelin T, Gordon J. 1979. Electrophoretic transfer of proteins from polyacrylamide gels to nitrocellulose sheets: procedure and some applications. *Proc. Natl. Acad. Sci. U. S. A.* **76**:4350–4354.

Velling T, Risteli J, Wennerberg K, Mosher DF, Johansson S. 2002. Polymerization of type I and III collagens is dependent on fibronectin and enhanced by integrins alpha 11beta 1 and alpha 2beta 1. *J. Biol. Chem.* **277**:37377–37381.

Villeda-Hernandez V, Barroso R, Mendez M, Nava C, Huerta R, Rios C. 2001. Enhanced brain regional lipid peroxidation in developing rats exposed to low level lead acetate. *Brain Res. Bull.* **55**:247–251.

Wallace K, Burt AD, Wright MC. 2008. Liver fibrosis. *Biochem. J.* **411**:1–18.

Wells RG. 2000. Fibrogenesis. TGF-b signaling pathways. *Am. J. Physiol. Gastrointest. Liver Physiol.* **279**:G845–G850.

Wells RG. 2006. Mechanisms of liver fibrosis: new insights into an old problem. *Drug Discov. Today Dis. Models* **3**:489–495.

Wells RG. 2008. Cellular sources of extracellular matrix in hepatic fibrosis. *Clin. Liver Dis.* **12**:759–768

Wynn TA. 2008. Cellular and molecular mechanisms of fibrosis. *J. Pathol.* **214**:199–210.

Xu ZJ, Fan JG, Ding XD, Qiao L, Wang GL. 2010. Characterization of high-fat, diet-induced, non-alcoholic steatohepatitis with fibrosis in rats. *Dig. Dis. Sci.* **55**:931–940.

Zhang J, Wang XF, Lu ZB, Liu NQ, Zhao BL. 2004. The effects of meso-2,3-dimercaptosuccinic acid and oligomeric procyanidins on acute lead neurotoxicity in rat hippocampus. *Free Radic. Biol. Med.* **37**:1037–1050.

Zhang C, Zhu Y, Wan J, Xu X, Shi H, Lu X. 2006. Effects of Ginkgo biloba extract on cell proliferation, cytokines and extracellular matrix of hepatic stellate cells. *Liver Int.* **26**:1283–1290.